An anthropomorphic polyvinyl alcohol brain phantom based on Colin27 for use in multimodal imaging

Sean Jy-Shyang Chen[a)]
McConnell Brain Imaging Centre, Montreal Neurological Institute, McGill University, Montreal H3A 2B4, Canada

Pierre Hellier
INRIA Rennes, EPI Serpico, IRISA, F-35042 Rennes, France

Maud Marchal
INRIA Rennes, Bunraku, IRISA-INSA, F-35042 Rennes, France

Jean-Yves Gauvrit
INRIA VisAGes U746, IRISA, F-35042 Rennes, France; INSERM U746, IRISA, F-35042 Rennes, France; and Université de Rennes 1, 35065, Rennes, France

Romain Carpentier
INRIA VisAGes U746, IRISA, F-35042 Rennes, France

Xavier Morandi
INRIA VisAGes U746, IRISA, F-35042 Rennes, France; INSERM U746, IRISA, F-35042 Rennes, France; and Université de Rennes 1, 35065 Rennes, France

D. Louis Collins
McConnell Brain Imaging Centre, Montreal Neurological Institute, McGill University, Montreal H3A 2B4, Canada

(Received 28 April 2011; revised 6 December 2011; accepted for publication 7 December 2011; published 3 January 2012)

Purpose: In this paper, the method for the creation of an anatomically and mechanically realistic brain phantom from polyvinyl alcohol cryogel (PVA-C) is proposed for validation of image processing methods such as segmentation, reconstruction, registration, and denoising. PVA-C is material widely used in medical imaging phantoms because of its mechanical similarities to soft tissues.
Methods: The phantom was cast in a mold designed using the left hemisphere of the Colin27 brain dataset [C. Holmes *et al.*, "Enhancement of MR images using registration for signal averaging," J. Comput. Assist. Tomogr. **22**(2), 324 (1998)]. Marker spheres and inflatable catheters were also implanted to enable good registration comparisons and to simulate tissue deformation, respectively.
Results: The phantom contained deep sulci, a complete insular region, and an anatomically accurate left ventricle. It was found to provide good contrast in triple modality imaging, consisting of computed tomography, ultrasound, and magnetic resonance imaging. Multiple sets of multimodal data were acquired from this phantom.
Conclusions: The methods for building the anatomically accurate, multimodality phantom were described in this work. All multimodal data are made available freely to the image processing community (http://pvabrain.inria.fr). We believe the phantom images could allow for the validation and further aid in the development of novel medical image processing techniques. © *2012 American Association of Physicists in Medicine*. [DOI: 10.1118/1.3673069]

Key words: PVA, brain phantom, Colin27, anthropomorphic, image datasets

I. INTRODUCTION

The human cerebrum is a topologically complex organ with deep fissures and sulci over its lateral and medial surfaces, as well as fluid filled ventricles of complex shape and form in its interior. The creation of a physical model capable of depicting the form of the cerebrum is not trivial due in part to these deep structures. Previous works in creating brain phantoms have either reduced the depth of the sulci,[2] or only recreated the form of the brain superficially with dessert gelatin molds.[3,4] Although these phantoms bear a cursory resemblance to the human cerebrum, they do not accurately depict the gross anatomy of the brain. Registering these phantoms to their acquired multimodality images may also not be straightforward since the landmarks on the phantom are not easy to find or image. This may be due to the structures being smaller than the imaging resolution or because of insufficient contrast of the markers with respect to its surroundings. For instance, Reinertsen and Collins[4] relied on the presence of bubbles in their phantom to act as landmarks for validation of their phantom. While trapped bubbles can be useful as landmarks in phantom validation, their locations cannot be controlled. Even when the bubbles are present, they may also be difficult to identify uniquely. To address

these issues, multimodal landmarks need to be placed in the phantom.

The objective of this study is to create a triple modality human brain phantom with anatomically realistic structures and mechanical properties such as firmness, stiffness, and elasticity approaching that of a live human brain. Henceforth, we will collectively refer to these properties as "texture." The material selected for constructing this phantom is polyvinyl alcohol (PVA), which is a polymer synthesized from polyvinyl acetate by hydrolysis of their acetate groups.[2] PVA is commonly used in industrial products such as adhesives, strengtheners for fiber products, thickeners for paints and other liquids, as well as in for the creation of films, emulsions, and coatings for various engineering purposes.[4,5] When liquid PVA solutions undergo a specified period of freezing at a set temperature and are then allowed to thaw slowly to room temperature, this freeze-thaw cycle (FTC) transforms the liquid PVA solution into a elastic semi-opaque gel know as polyvinyl alcohol cryogel (PVA-C).[6–9]

In previous studies, soft tissue phantoms made from PVA-C have been used to develop, characterize, and refine different imaging or image processing methods.[10–12] PVA-C is a good material for such studies since it has similar texture, mechanical properties such as compressibility and elasticity, and similar water content to many soft tissues.[2,4,10–14] PVA-C has many other desirable characteristics for building phantoms. For example, its tensile strength allows it to be stretched 5–6 times its original dimensions without tearing or rupturing, while its high degree of elasticity lets it return to its original shape with little permanent deformation.[8,14] With cold storage and the addition of biocides, PVA is also relatively tough and long-lasting when compared with other similar textured materials such as gelatin or agar.[13,14] PVA-C is also safe for normal handling in that it is biocompatible and nontoxic.[13] Finally, the gelling and setting of PVA into PVA-C is relatively uninvolved, requiring only the freezing and thawing of the molded PVA solution.

For these reasons, PVA-C has been used in the construction of soft tissue phantoms and to study a wide variety of tissues including those of the heart,[15,16] breast,[11,12,17] prostate,[14] arterial vasculature,[2,9,18] and brain,[2,4] in addition to lesions and tumors within these tissues.[11,12,14] In the following sections, we describe the methods we used to create our brain phantom. We seek to contribute to the literature a phantom that has:

Anatomical accuracy: Deep cortical structures of the Colin27 cerebrum, such as the sulci, the insular region and the ventricles are realistically represented in the cast phantom.

Realistic texture: Recipes of PVA-C with textures approaching that of live human cerebral tissues were determined through the feedback of a neurosurgeon who knows the texture of the human brain and tumor tissues.

Multimodal imaging: A single phantom that can be imaged effectively in computed tomography (CT), ultrasound (US), and magnetic resonance (MR) modalities with good contrast between phantom and water as well as between the phantom and its implants.

Freely available data: Images acquired using the US, MR, and CT scanners are made available through our website to researchers and the general public. Images for this phantom were acquired using magnetic resonance imaging [T1 and T2 weighted, proton density (PD), fluid attenuated inversion recovery (FLAIR), and diffusion tensor imaging (DTI)], ultrasound imaging, and computed tomography, to ensure that the phantom exhibits similar contrast to images of the live cerebrum acquired using these imaging modalities.

We also embedded inflatable catheters in the manner of Reinertsen *et al.*[3] to simulate deformation from brain-shift, which is caused by the nonlinear distortion of brain tissue due to gravity and brain swelling from various physiological factors.

Potentially any PVA-C formula can be used to cast the brain phantom provided that it can be easily removed from the mold and that it holds its form once unmolded. However, we have noticed in past experiments that attaining the right phantom texture is important in getting realistic deformation through catheter inflation. As such, we believe that a PVA-C formulation that approximates live brain texture is desirable for the construction of our anatomically accurate phantom in order to validate nonlinear image registration algorithms and other image processing methods. Furthermore, the PVA-C formulation must be able to suspend the contrast agents used in the phantom (i.e., without settling out) during the casting of the phantom.

As such, although an imaging phantom will not necessarily need to have both anatomical accuracy and a realistic texture, in this work, we strove to incorporate both of these requirements into our phantom.

In Material and Methods, we describe the methods for preparing the PVA-C material, the added contrast agents, the creation of the phantom mold, and our multimodal image acquisition of the phantom. We conclude the paper with a listing of our Results followed by a Discussion of the work.

II. MATERIAL AND METHODS

II.A. Preparing PVA-C

The PVA solutions used to cast the PVA-C brain phantom and its various components were prepared using 99%–100% hydrolyzed PVA with an average molecular weight of 86 kDa from Acros Organics (Geel, Belgium; Code:418120010).

Master PVA solutions were prepared in large quantities by combining heated distilled water of a certain mass with PVA solute of another mass. The final mass of PVA solute will make up a specific percentage of final solution's mass. This is known as mass percentage and is commonly abbreviated as w/w. In our experiments, master PVA solutions of 5 and 8% (w/w) were prepared.

The mixture was constantly stirred until the PVA particles are well hydrated upon which the holding vessel of PVA and water mixture was placed in an oven of 93–95 °C for several hours. This ensures temperature homogeneity in the liquid and that the PVA granules dissolve properly. We were also careful to keep the temperature of the holding vessels below 100 °C to minimize water loss and the formation of polymer films on the liquid surface. These parameters were taken from the solution preparation guidelines of Celvol PVA of a similar grade to what we were using.[5]

The finished master solutions were checked visually to ensure that all PVA granules had been dissolved. Small quantities of distilled water were added back into the solutions according to the amounts lost during preparation of the PVA solution. From these PVA master solutions, base solutions of lower mass percentages could be produced by heating the master solution and mixing in additional water.

PVA-C was polymerized from a PVA solution by completely freezing and thawing the solutions, which results into semitransparent flexible gel. The PVA solutions were placed in a room temperature (25 °C) chest freezer and cooled to between −25 °C and −20 °C. After 12 h of freezing at the aforementioned temperatures, the freezer was stopped and its interior was allowed to rise back to room temperature over another 12 h period. The cycles were varied from 1 to 3 FTCs to produce a range of different PVA-C texture consistencies.

II.B. Choosing a PVA-C Formula

In order to select a PVA-C formula (PVA solution concentration and FTC) that would provide a texture similar to that of a live human brain in our deformable brain phantom, we employed the subjective assessment of a neurosurgeon with 21 years of experience in vascular and skull base surgery, who was familiar with the texture of the human brain and its pathologies. The surgeon was asked to palpate an array of PVA-C samples that had been prepared with either 1, 2, or 3 FTCs and 4%, 5%, 6%, or 8% PVA solutions (12 PVA-C samples in total; see Fig. 1). During this exercise, the samples were palpated at room temperature by the neurosurgeon while gloved and blindfolded. The neurosurgeon was asked rate the similarity of each sample to human brain tissue on a scale of 0 (least similar) to 10 (most similar). The aforementioned procedure was then repeated to choose the samples which felt most like low grade gliomas.

We note that this strategy for selecting a PVA-C formula is subjective and cannot be used to draw conclusions about the quantitative rheological properties of live human brain tissue beyond the needs our tests. These properties should be measured and quantified using elastography or more directly through intraoperative mechanical tests. Along with additional information from the formal characterization of the rheological parameters of our PVA-C samples, we should be able to better select a PVA formula that is quantitatively similar to the mechanical properties of human brain.

FIG. 1. Samples of PVA-C from 4%–8% (left to right) and 1–3 freeze-thaw-cycles (top to bottom). Note that the samples that have undergone 1 freeze-thaw-cycle (FTC) samples are more translucent than higher FTC samples. Note that the 4% 1 FTC sample deforms significantly under its own weight.

II.C. Triple modality contrast agents

Commonly available chemicals were used to change the contrast between the phantom and water for all modalities (US, MR, and CT). A PVA-C with the PVA concentration and FTC resembling textures similar to a living human cerebrum was chosen to be the base solution for dissolving the contrast enhancing chemicals. We list all quantities of contrast medium added to the PVA solution as mass percentages (w/w) of the chosen PVA solution.

To increase backscattering of sound waves in US imaging, solutions containing talcum powder at 4%, 2%, 1%, and 0.5% weight of the base solution were mixed. Other materials such as thin-layer chromatography grade silica gel[14] and cellulose,[13] along with enamel paint[16] have also been used as acoustic backscatterers but we found that commercial grade talcum powder also performs well. Each of the samples were immersed in water, imaged, and then visually examined for contrast with the surrounding water and implanted PVA markers spheres.

For increasing phantom contrast in CT imaging, a powdered barium sulfate ($BaSO_4$) preparation used for colon enema (Guerbet Micropaque Colon, Guerbet, Villepinte, Île-de-France, France) was mixed into our PVA solutions. Although $BaSO_4$ at concentrations greater than 60% can drastically alter MR relaxation time, lower concentrations of around 1%–8% do not appear to significantly alter MR relaxation times or interfere with image signal.[19] Solutions were prepared with 8%, 6%, 3%, and 1% w/w $BaSO_4$ of the initial base solution.

To enhance the signal in T1 weighted images, copper sulfate ($CuSO_4$) was added to the PVA mixture in small quantities. $CuSO_4$ has been widely used as a MR contrast agent since the late 1970s in phantoms used for MR performance validation such as the recently developed Alzheimer's Disease Neuroimaging Initiative (ADNI) phantom.[20] Minute quantities of $CuSO_4$ dramatically increase the contrast of the PVA sample in T1 and T2 weighted images. To find an optimal concentration of $CuSO_4$, we prepared 0.2%, 0.1%, 0.05%, and 0.025% (w/w) anhydrous $CuSO_4$ PVA-C samples and imaged them with T1 and T2 imaging sequences.

The appropriate concentrations of talcum, $BaSO_4$, and $CuSO_4$ were determined by choosing the PVA-C samples that had the least amount of contrast agent but still gave qualitatively good MR, CT, and US contrast when the PVA-C samples were imaged when submerged in water in a closed container.

II.D. Phantom construction

II.D.1. Brain mold

The mold for our brain phantom was based on the left hemisphere of the Colin-27 data set.[1] The cortical surface of the left hemisphere was segmented using Freesurfer[21] to

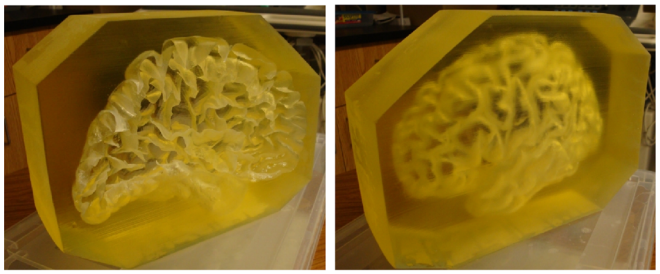

A B

FIG. 2. Two views of the flexible phantom mold from (A) the inside and (B) the outside.

produce a polygonal surface mesh, which was then processed using the butterfly subdivision module in MESHLAB (Ref. 22) to refine the cortical surface represented by the mesh and also reduce the number of facets in the mesh.

We then subtracted this processed cortical surface mesh from a rectangular prism mesh using the boolean operator in Blender3D,[23] in order to create a "negative" of the cortical surface for fabricating our brain mold. After manually correcting the polygonal mesh model for holes, unconnected mesh fragments, and inverse surface normals, the model was then saved in the STL file format, which is commonly used for stereolithographic printing.

We utilized the services of RedEye On Demand (Eden Prairie, MN, USA) for the fabrication of our brain phantom mold using the TangoPlus Polyjet Resin (FC-930) as the material. This clear photopolymer was deposited layer by layer in order to produce a finished three dimensional object (see Fig. 2). We found that the mold made using this rubbery material was able to accurately model the sulci and insular region of the cerebral hemisphere while having enough flexibility to allow the PVA-C to be unmolded without damaging the phantom or the mold itself. The mold reverts itself to its original shape when deformed.

The bottom of a plastic tub was cut out and glued around the opening of the flexible rubber mold. This allowed us to cast a base for our phantom when unmolded and also limited its relative movement when placed and imaged in another plastic tub of the same size and format.

The mold component for the left ventricle of the phantom was constructed separately using silicone bathroom caulk. Layers of caulk approximately 2 mm thick were applied to vellum traces from life-size printouts of segmented 2 mm sagittal sections of the left ventricle. These layers were then assembled medially to laterally and aligned using crosshairs on the printout traces to maintain placement accuracy of the sagittal sections and then covered with additional silicone rubber caulk to smooth the mold component surface (see Fig. 3).

A B

FIG. 3. The silicone rubber and cellulose composite mold component used to cast the fluid filled left ventricle in our phantom (A) before and (B) after being covered with additional silicone caulking to smooth the surface.

II.D.2. Implants

To make our phantom useful for tests in image guidance and registration, various structures created from various grades of PVA-C were included into the phantom.

To create spherical registration targets/landmarks, we used a harder PVA-C made from 8% PVA solution that has undergone 2 FTC containing high quantities of contrast agents described in Sec. II C for a strong contrast. We found this PVA-C formula to be suitable since it is relatively firm and will not change its shape significantly with phantom deformation. These were molded using the containers for reflective passive spheres used in optical tracking. By using a firmer PVA-C, we limited the amount of distortion that the structure can undergo while enabling the targets to be imaged by US, MR, and CT. These spheres are approximately 11–12 mm in diameter. Together with the phantom cortex landmarks, these internal targets can be used as gold standard markers to verify registration accuracy in the three imaging modalities (see Fig. 4). The spheres can be imaged well with ultrasound since they do not have strong specular reflection due to its similar texture to the surrounding PVA-C tissue. This allowed them to be imaged with relatively even contrast from the edge of the sphere to the center. Furthermore, it prevents the heavy US shadowing of the tissues located "behind" the sphere.

A PVA-C "tumor" was also created using 4% PVA solution with 1 FTC and then embedded into the phantom. The tumor was molded using the ovoid plastic case from inside a Kinder surprise egg (Ferrero, Pino Torinese, Italy). A small hole was drilled on one of the poles of the egg to allow for expansion during the FTC. The tumor was then placed in the phantom in order to test guidance accuracy in surgical procedures and also to provide another tissue in the phantom of different texture and contrast.

FIG. 4. The 11–12 mm diameter multimodal spherical markers implanted into our phantom

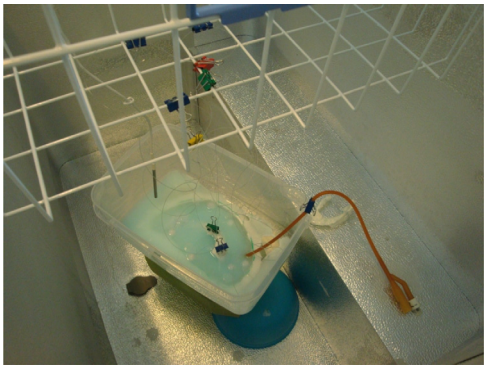

FIG. 5. The setup for casting the hemispheric portion of the phantom. After the hemispheric part is well frozen, the clamps are removed and PVA solution for casting the base is poured into the mold.

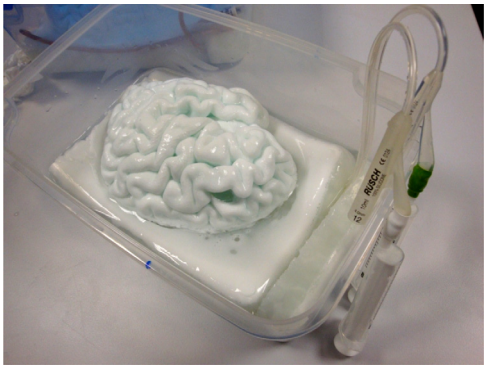

FIG. 6. The PVA-C phantom casted from our Colin27 based brain phantom mold being prepared for scanning. Note the deep sulci and insular regions of the phantom and the ends of the catheters used to inflate the phantom on the right. For most of our scans, the plastic tub was filled with just enough water to cover the top of the brain phantom.

II.D.3. Phantom casting

The main brain phantom tissue was cast using the optimal liquid PVA-C identified in the experiments described in Sec. II B combined with the contrast agent concentrations selected in Sec. II C. The mixture was poured into the brain mold and any air or bubbles trapped in the sulci are removed such that cavities do not form in the sulcal or gyral surfaces of the phantom.

The PVA-C landmark spheres and tumor implants were skewered and suspended using 0.45 mm monofilament fishing lines inside the filled phantom mold at their desired location. The left ventricle mold component was clamped and also suspended with fishing lines in a similar fashion. We found that this technique allowed good positioning of the structures and prevented them from sinking to the bottom of the mold. (see Fig. 5).

Finally, we placed the inflatable head of a urinary catheter into the frontal lobe of the phantom and another in the medial portion of the phantom in the cast base of the mold. Each urinary catheter could be inflated with up to 10 ml of water using a syringe in the manner described by Reinertsen and Collins.[4] This allowed us to vary the extent of deformation on the phantom and conduct experiments on the accuracy of various nonlinear registration algorithms.

The entire phantom casting setup was then frozen solid. A thick base for the phantom was cast by pouring an approximately 3 cm thick layer of clear 8% PVA solution over the frozen phantom, which produces a thick layer of PVA-C in the completed phantom of the same thickness. Everything was then allowed to freeze completely over the course of 24 h. Once thawed, the brain phantom readily detaches from the sides of the mold and recovered their original form. An example of the completed phantom can be seen in Fig. 6.

II.E. Imaging

II.E.1. Modalities and parameters

Our triple modality imaging includes acquisition of phantom images in MR, CT, and US. All our MR images were acquired on a Siemens Verio 3T MR scanner (Siemens Healthcare, Erlangen, Germany) using the imaging parameters listed in Table I.

CT images of the phantom were acquired for the phantom in 491 axial slices at 1.25 mm thickness using a GE LightSpeed 16 VCT scanner (GE Healthcare, Little Chalfont, Buckinghamshire, UK).

US images were acquired with a Sonosite 180 Plus (Sonosite, Bothell, WA, USA) diagnostic ultrasound system tracked using a Medtronic Stealth neurosurgical station (Medtronic, Minneapolis, MN, USA). Images for the phantom were acquired as a series of tracked B-mode US images of 44 images in 4–6 sweeps at either 5.2 or 7.1 cm depth.

II.E.2. Acquisition methodology

The images of the deformed phantom were acquired in the following manner. A series of images were first acquired for each of the CT, US, multiple MR modalities mentioned. After the image acquisition, the phantom was deformed and then a series of acquisitions with the same imaging parameters was repeated. Deformation is done by inflating each of the two implanted urinary catheters in the phantom (see Fig. 6) with 0, 5, or 10 ml of water through five rounds of inflations in the manner described in Table II. For each given amount of deformation, the phantom was scanned in all the

TABLE I. The MR modalities used to image the phantom with deformation and their imaging parameters. The modalities used are: T1-weighted spin-echo (T1-SE), T1-weighted gradient-echo (T1-GE), T2-weighted gradient-echo (T2-GE), proton density (PD), fluid attenuated inversion recovery (FLAIR), and diffusion weighted imaging (DWI). The sequences each have their own repetition times (TR) and echo times (TE), as well as an additional inversion time (TI) for FLAIR imaging. Following the acquisition of the DWI 30 directions, the fractional anisotropy (FA), apparent diffusion coefficient (ADC), and trace weighted images (TWI) were computed.

MR Modality	TR (ms)	TE (ms)	Flip angle (deg)	Voxel size (mm^3)
T1-SE	668	8.9	70	$1 \times 1 \times 3$
T1-GE	1900	3	9	1 isotropic
T2-GE	6530	840	150	$1 \times 1 \times 3$
PD	6530	9.4	150	$1 \times 1 \times 3$
FLAIR (TI = 1800 ms)	5000	273	120	1 isotropic
DWI	9300	94	90	$1 \times 1 \times 2$

TABLE II. The inflation volumes on Catheters 1 and 2 used to deform the brain phantom on the five multimodality imaging series.

Series	Catheter 1 (ml)	Catheter 2 (ml)
1	0	0
2	5	0
3	5	5
4	5	10
5	10	10

modalities without changing the inflation of the catheters. This ensures that exactly the same physical deformations were scanned in each modality. It is only after the whole series of the multimodal images were acquired for a deformation, that the catheter inflations were changed.

Images for testing super-resolution image processing and scan-rescan reliability testing, were acquired by scanning the phantom without catheter inflation using MP-RAGE T1 weighted gradient-echo sequence (TR = 1900 ms, TE = 3 ms, Flip angle = 9°, 1 mm isotropic). This acquisition was repeated 10 times with water and 10 times without water. Each of these scans were acquired at an isotropic resolution of 0.5 mm, with the phantom displaced slightly (<1 cm) between each of the acquisitions.

II.E.3. Postprocessing

Following the data acquisition, the US images were reconstructed into an US volume using distance weighted interpolation and denoised using the nonlocal means method described in Coupé *et al.*[24] Transformation from the tracked US probe given by the neuronavigation system were used to reslice all the MR and CT volumes to match each reconstructed 3D US volume.

The MR T1 and T2 times of tissues in our phantom were determined using software available from our institute.

III. RESULTS

III.A. PVA-C formula choice

Based on the neurosurgeon's PVA-C scoring (see Table III), we selected two samples for further analysis:

- 6% PVA with 1 FTC
- 4% PVA with 2 FTC

We found that a large quantity of the contrast agents tended to settle to the bottom of the large brain mold while freezing the 4% PVA mixture. We therefore choose to build the normal brain phantom tissue with 6% PVA with 1 FTC. The low grade glioma tissue was made using 4% PVA with 3 FTCs, as it was determined to be the best representative sample by the surgeon. In order to further justify our choice for the PVA-C formula used for the normal phantom tissue, a PVA-C sample of 6% PVA 1 FTC was submitted for rheological testing on a 3369 Dual Column system (Instron, Norwood, MA, USA). While only one PVA-C sample was tested, we found that the Young's modulus for the sample was 4.6 kPa ± 0.5%, which is in the range found for human brain.[25]

TABLE III. PVA sample texture ratings for similarity to live human cerebral tissue by the neurosurgeon who specializes in neurovascular surgery with 21 years experience The samples were rated from 0 to 10 with the former being dissimilar to brain tissue and the latter being exactly like brain tissue.

	4% PVA	5% PVA	6% PVA	8% PVA
1 FTC	0	4	7	4[a]
2 FTC	8	5	0	0
3 FTC	6[a]	0	0	0

[a]This indicates a sample that the surgeon believed felt like a low grade gliomas.

III.B. Triple modality contrast

We used the 6% 1 FTC PVA-C formula as the base material to test different concentrations of $BaSO_4$, $CuSO_4$, and talcum powder contrast agent. These different PVA-C samples were then scanned using MR, CT, and US imaging. We found that for the phantom brain tissue, concentrations of 2% $BaSO_4$, 0.025% $CuSO_4$, and 1% talcum as contrast agents worked well for CT, MR, and US, respectively. Through only palpation tests done by the neurosurgeon and the authors, we determined that the texture of the PVA-C did not change perceivably with the addition of these quantities of contrast agents.

For our triple modality image markers, we found that 5% $BaSO_4$, 0.2% $CuSO_4$, and 5% talcum as contrast agents in 8% PVA with 2 FTC provided adequate contrast for CT, MR, and US, respectively. These contrast concentrations were chosen to provide the markers with sufficient contrast from the surrounding normal tissue PVA-C as to be easily visible on the images of each modality.

III.C. Imaging results

A sample of the multimodal images and the result of the inflations can be seen in Figs. 7 and 8, respectively.

The MR and CT Images aligned and resliced to the US using tracking information given by the neuronavigation system can be seen in Figs. 9(a) and 9(b), respectively. The corresponding 2D US image can be seen in Fig. 9(c).

The MR T1 and T2 times of tissues in our phantom were determined using software available from our institute. T1 and T2 times for the phantom tissue were 1004–1213 ms and 163–182 ms, respectively, while T1 and T2 times for the casted tumor were 1900–2600 ms and 1100–1665 ms, respectively.

IV. DISCUSSION

IV.A. Image processing validation

We believe that the acquired multimodal images with different deformations can be used for validation of many image processing techniques such as segmentation, image reconstruction, linear or nonlinear registration, and denoising algorithms, using images acquired from one modality to act as the ground truth of another. The deformation images can also be used to validate physical simulation.

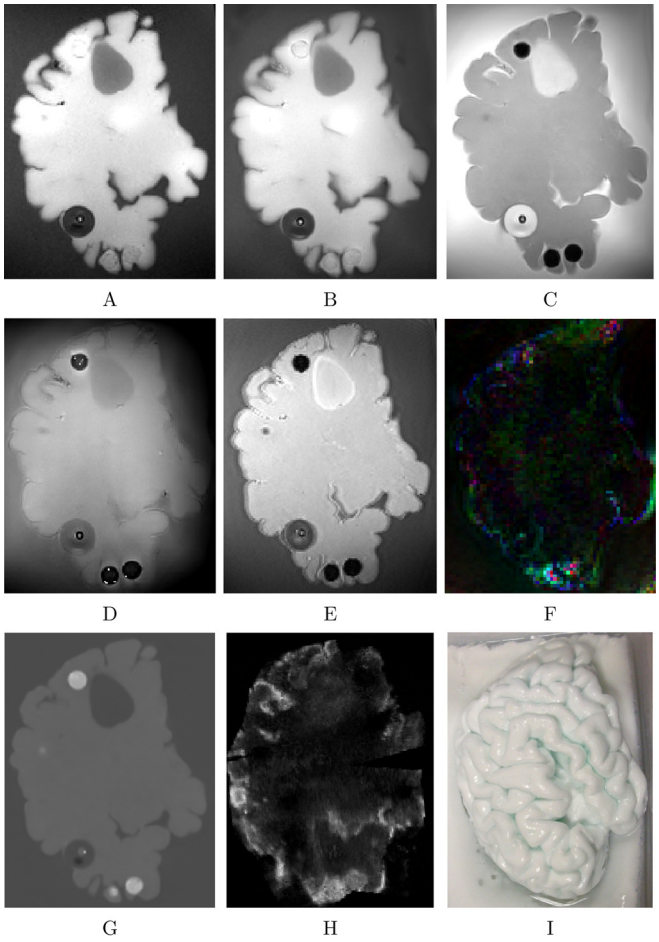

FIG. 7. A selection of PVA-C brain phantom images acquired using MR T1-weighted gradient-echo(A), MR T1-weighted spin-echo (B), MR T2-weighted (C), MR PD (D), MR FLAIR (E), MR DTI colour map (F), CT (G), a reconstructed US image (H), and a picture of the PVA-C Phantom (I).

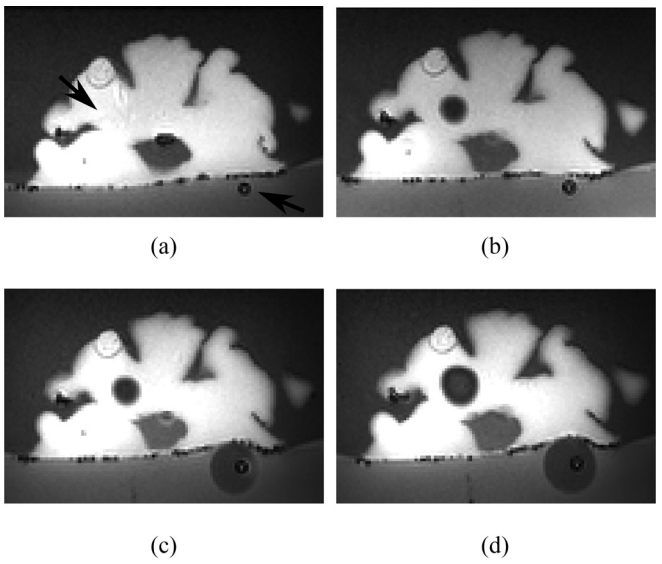

FIG. 8. Images (a)–(b) shows the same coronal slice of the phantom imaged with T1-weighted gradient-echo at different inflations (series 1, 2, 3, and 5, of Table II, respectively). The arrows in image (a) show the location of the catheters in that slice of the phantom.

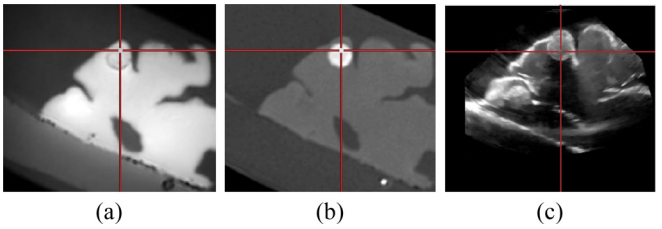

FIG. 9. Images (a)–(c) show a cropped section of the phantom MR and CT images aligned with the US image.

As well, the multiple displacement MR images can be used to validate the accuracy of super-resolution algorithm, which can use the information from image redundancies and subpixel shifts in low resolution images to recreate a higher resolution image of the original imaged object. Further information on super-resolution methods can be found in Manjón *et al*.[26]

In addition, the phantom may be used for testing and training of stereotatic procedures. such as biopsy needle insertions or deep-brain stimulator placement. Together with the phantom's accurate gross cortical anatomy, its similarity to the texture of live brain, and its low cost, the phantom can be useful educational tool in training medical professionals.

IV.B. Limitations and future work

There are several limitations in the current phantom that could be addressed in future work. Notably, our method for selecting the PVA solution concentration and the number of FTCs relies on a subjective assessment. A better approach may be to measure the rheological characteristics of live human brain tissue using MR or US elastography or through direct intraoperative mechanical characterization and use these results to guide the choice of PVA concentration and number of FTCs. This would allow for the ability to select the PVA concentration and FTC as a function of the desired physical and imaging properties of the material. Experiments quantifying the rheological properties of human brain will have to account for the physiological state of the individual patient since different factors such as blood pressure, the administration of pharmaceuticals (e.g., mannitol), or other physiological conditions[27] can dramatically change the rheological properties of the human brain.

Nevertheless, the concentration and number of freeze-thaw cycles chosen in this study resulted in a texture that was qualitatively comparable to live brain tissue when palpated by an experienced neurosurgeon. Moreover, the phantom created here had rheological characteristics that were similar to those found in the literature in terms of Young's modulus for live human brain and it deforms more realistically than previously proposed deformable brain phantoms in the literature.

The phantom proposed in this study could also be improved by devising a method of simulating heterogeneous tissue, since the current version only allows for homogeneous simulated tissue with discrete punctuate insertions. Doing this would make it possible to simulate different brain tissues (e.g., white matter, cortical grey matter, deep grey matter). More sophisticated phantom casting techniques

would also make it possible to simulate white matter tracts and blood vessels.

Finally, it was found that over time the $CuSO_4$ MR contrast agents tended to diffuse or leak from the landmark spheres into the surrounding tissue. This difficulty could be resolved either by sealing the landmark spheres to eliminate leaking, or find MR contrast agents that will not diffuse out of the spheres.

V. CONCLUSIONS

We have presented a method for creating an anthropomorphic human brain phantom that is anatomically and mechanically realistic, which can also be effectively imaged in the multiple modalities of MR, CT, and US imaging.

We have also made all the images acquired from the phantom publicly available to the larger image processing community (http://pvabrain.inria.fr). The phantom and data will enable validation of image processing methods and facilitate the development of new interventional methods.

ACKNOWLEDGMENTS

The authors would like to thank the Neurinfo platform team for its financial support and their assistance in processing and acquiring the MR data, as well as Professor Olivier Le Guillou and Florence Le Dret at the chemistry department of the Institut National des Sciences Appliquées (INSA) de Rennes for allowing us to use their equipment for preparing solutions. The authors are also grateful to the Fonds québécois de la recherche sur la nature et les technologies (FQRNT) and the Collège Doctoral International (CDI) de l'Université européenne de Bretagne (UEB) Bourse de Mobilité Internationale Entrante for funding this project.

[a]Author to whom correspondence should be addressed. Electronic mail: sjschen@bic.mni.mcgill.ca

[1]C. Holmes, R. Hoge, L. Collins, R. Woods, A. Toga, and A. Evans, "Enhancement of MR images using registration for signal averaging," J. Comput. Assist. Tomogr. **22**(2), pp. 324–333 (1998).

[2]K. J. M. Surry, H. J. B. Austin, A. Fenster, and T. M. Peters, "Poly(vinyl alcohol) cryogel phantoms for use in ultrasound and MR imaging," Phys. Med. Biol. **49**(24), 5529–5546 (2004).

[3]I. Reinertsen, M. Descoteaux, S. Drouin, K. Siddiqi, and D. L. Collins, "Vessel driven correction of brain shift," *MICCAI 2004*, pp. 208–216 (2004).

[4]I. Reinertsen and D. L. Collins, "A realistic phantom for brain-shift simulations," Med. Phys. **33**(9), 3234–3240 (2006).

[5]Sekisui Specialty Chemicals, Celvol Polyvinyl Alcohol… Solution Preparation Guidelines, Sekisui Specialty Chemicals U.S., 1603 West LBJ Freeway, Dallas, TX, 2009.

[6]N. A. Peppas, "Turbidimetric studies of aqueous poly(vinyl alcohol) solutions," Die Makromolekulare Chemie **176**(11), 3433–3440 (1975).

[7]S. R. Stauffer and N. A. Peppas, "Poly (vinyl alcohol) hydrogels prepared by freezing-thawing cyclic processing," Polymer **33**(18), 3932–3936 (1992).

[8]N. A. Peppas and S. R. Stauffer, "Reinforced uncrosslinked poly (vinyl alcohol) gels produced by cyclic freezing-thawing processes: A short review," J. Controlled Release **16**(3), 305–310 (1991).

[9]K. C. Chu and B. K. Rutt, "Polyvinyl alcohol cryogel: An ideal phantom material for MR studies of arterial flow and elasticity," Magn. Reson. Med. **37**(2) 314–319 (1997).

[10]F. Duboeuf, A. Bbasarab, H. Liebgott, E. Brusseau, P. Delechartre, and D. Vray, "Investigation of PVA cryogel Young's modulus stability with time, controlled by a simple reliable technique," Med. Phys. **36**(2), 656–661 (2009).

[11]H. Mehravian and A. Samani, in *Constrained hyperelastic parameters reconstruction of PVA (Polyvinyl Alcohol) phantom undergoing large deformation*, edited by M. I. Miga and K. H. Wong [Medical Imaging 2009: Visualization, Image-Guided Procedures, and Modeling **7261**(1), 72612G (2009)] (SPIE, Lake Buena Vista, FL, 2009).

[12]S. Manohar, A. Kharine, J. C. G. van Hespen, W. Steenbergen, and T. G. van Leeuwen, "Photoacoustic mammography laboratory prototype: Imaging of breast tissue phantoms," J. Biomed. Opt. **9**(6), 1172–1181 (2004).

[13]J. Fromageau, J.-L. Gennisson, C. Schmitt, R. Maurice, R. Mongrain, and G. Cloutier, "Estimation of polyvinyl alcohol cryogel mechanical properties with four ultrasound elastography methods and comparison with gold standard testings," IEEE Trans. Ultrason. Ferroelectr. Freq. Control **54**(3), 498–509 (2007).

[14]W. Khaled, T. Neumann, H. Ermert, S. Reichling, A. Arnold, and O. Bruhns, "Evaluation of material parameters of PVA phantoms for reconstructive ultrasound elastography," *IEEE Ultrasonics Symposium*, pp. 1329–1332 (2007).

[15]B. Lesniak-Plewinska, M. Kowalski, S. Cygan, E. Kowalik, and K. Kaluzynski, "Experimental setup with dual chamber cardiac phantom for ultrasonic elastography," *4th European Conference of the International Federation for Medical and Biological Engineering*, pp. 559–562 (2009).

[16]C. Jia, K. Kim, T. Kolias, W. Weitzel, J. Rubin, and M. O'Donnell, "Left ventricular phantom with pulsatile circulation for ultrasound strain rate imaging," *IEEE Ultrasonics Symposium*, pp. 1317–1320 (2006).

[17]K. J. M. Surry, W. L. Smith, L. J. Campbell, G. R. Mills, D. B. Downey, and A. Fenster, "The development and evaluation of a three-dimensional ultrasound-guided breast biopsy apparatus," Med. Image Anal. **6**(3), pp. 301–312 (2002).

[18]D. Dumont, E. Miller, J. Allen, C. Moyer, S. Hsu, and G. Trahey, "Peripheral vascular ARFI imaging: phantom and clinical results," *Ultrasonics Symposium, 2005 IEEE*, Vol. 1, pp. 605–608 (2005).

[19]H. I. Litt and A. S. Brody, "BaSO4-loaded agarose: A construction material for multimodality imaging phantoms," Acad. Radiol. **8**(5), 377–383 (2001).

[20]J. L. Gunter, M. A. Bernstein, B. J. Borowski, C. P. Ward, P. J. Britson, J. P. Felmlee, N. Schuff, M. Weiner, and C. R. Jack, "Measurement of MRI scanner performance with the ADNI phantom," Med. Phys. **36**(6), 2193–2205 (2009).

[21]B. Fischl, A. Liu, and A. Dale, "Automated manifold surgery: constructing geometrically accurate and topologically correct models of the human cerebral cortex," IEEE Trans. Med. Imaging **20**(1), 70–80 (2001).

[22]P. Cignoni, M. Callieri, M. Corsini, M. Dellepiane, F. Ganovelli, and G. Ranzuglia, "MeshLab: An Open-Source Mesh Processing Tool," *Sixth Eurographics Italian Chapter Conference*, pp. 129–136 (2008).

[23]www.blender.org.

[24]P. Coupé, P. Yger, S. Prima, P. Hellier, C. Kervrann, and C. Barillot, "An optimized blockwise non local means denoising filter for 3D magnetic resonance images," IEEE Trans. Med. Imaging **27**(4), 425–441 (2008).

[25]H. Metz, J. McElhaney, and A. K. Ommaya, "A comparison of the elasticity of live, dead, and fixed brain tissue," J. Biomech. **3**(4), 453–458 (1970).

[26]J. V. Manjón, P. Coupé, A. A. Buades, D. L. Collins, and M. A. Robles, "MRI superresolution using self-similarity and image priors," Int. J. Biomed. Imaging **2010**, 1–11 (2010).

[27]E. Walsh and A. Schettini, "Calculation of brain elastic parameters in vivo," Am. J. Physiol. Regulatory Integrative Comp. Physiol. **247**(4), R693–R7000 (1984).